Gain scheduled Linear Quadratic Regulator applied to the stabilization of a riderless bicycle

J. A. Brizuela-Mendoza[1], C. M. Astorga-Zaragoza[2], A. Zavala-Río[3], F. Canales-Abarca[4] and M. Martínez-García[1]

Abstract

In this paper, a gain scheduling control is designed to achieve the stabilization of a riderless bicycle. The main contribution is the design of a stabilizing control system including integral actions based on an observer and its corroboration through experimental results, with the objective of the stabilization of a riderless bicycle towards its upright position through a torque applied to the handlebar. The bicycle stabilization is achieved even when the translational velocity is varying over time, parameter considered as scheduling variable. The stabilizing system is based on an LQR gain scheduling control, concluding with the effective application of this scheme on a instrumented prototype.

List of notation

g	gravity acceleration
h	step width
j	indexing variable
r	reference signal
v	translational velocity
E_0, E_1	stiffness matrices
H	mass matrix
$K(v)$	velocity dependent control gain
$K_i(v)$	velocity dependent integral control gain
$L(v)$	observer gain
Q,R	LQR weighting matrix
T_δ	torque applied to handlebar
T_ϕ	torque applied to general frame
W	Damping matrix
α	LMI region parameter definition
δ	handlebar angle
θ	LMI region parameter definition
ϕ	roll angle
Φ	translational velocity interval set

Introduction

Nowadays, the interest of automatic control researchers in the bicycle dynamics is increasing. This is mainly due to the physical phenomena involved in the definition of the system, resulting in a control design problem motivating and challenging. This is referred to the fact that the open-loop (unforced) model is unstable, together with the under-actuated nature of the system, which generally induces unstable (zero) dynamics with respect to the usually measurable (output) variables. Another problem comes from the dependence of the vehicle dynamics on the time-varying translational velocity. Such characteristics render the control

design a non-trivial task. In particular, we focus on a riderless bicycle model, whose state-space representation involves the translational velocity explicitly. Thus, the dependence of the system on the time-varying parameter can be formulated in terms of a scheduling variable and, consequently, this paper presents the design and implementation of a gain scheduled control to ensure the upright position of a riderless bicycle while moving forward, by explicitly considering the time-varying translational velocity within the model. The main contribution of this paper is the design of a stabilizing control scheme including integral actions based on an observer and its corroboration through experimental results. Basically, the gain scheduling methodology involves designs to face problems related with non- linear systems, through linear control laws applicable over the entire operation region of the original system. This is done by means of a scheduling parameter directly involved in the definition of the operating point, which changes its value over time and, consequently, that of the operating point of the non-linear system. Thus, the scheduling parameter is assumed to be measurable, allowing the definition of the current operating point through a linear (local) model. As a result, a set of linear descriptions of the non linear system is computed by considering a time-varying scheduled parameter.[1] In addressing the

[1] Centro Universitario de los Valles, Universidad de Guadalajara, Ameca, Jalisco, Mexico.
[2] Tecnológico Nacional de Mexico Centro Nacional de Investigación y Desarrollo Tecnológico, Cuernavaca, Morelos, Mexico.
[3] Instituto Potosino de Investigación Científica y Tecnológica, San Luis Potosí, SLP., Mexico.
[4] ABB Corporate Research Center Brown, Baden-Datwil, Switzerland.

Corresponding author:
J. A. Brizuela-Mendoza. Centro Universitario de los Valles, Universidad de Guadalajara, Guadalajara-Ameca Km. 45.5, Ameca, Jalisco, Mexico.
Email: jorge.brizuela@valles.udg.mx

gain scheduling methodology, several works have been reported. For instance, the design of **a** gain-scheduled output-feedback control for LPV systems is addressed taking into account uncertainties on the scheduling parameters, computed considering H_∞ restrictions.[2] The problem of gain scheduling schemes has been reported for discrete-time LPV systems with a state feedback controllers.[3] Gain-scheduling and LPV controllers have been designed and applied to an active magnetic bearing system (AMB). In this work, taking the mass-imbalances as scheduling parameter, a set of H_∞ controllers are implemented to show experimental results by considering the Youla parametrization switching method.[4] It is important to note, on the other hand, that the features on gain scheduling allow its mixed implementation with other known control methodologies. For instance, a gain scheduled sliding mode control has been proposed and corroborated through simulations using a ship heading control system.[5] Another example is the design of an adaptive fuzzy gain scheduling PI controller, applied to a wind energy conversion system. This design considers fuzzy rules to adjust the parameters of the PI controller.[6] The problem of maximum power point tracking for a photovoltaic system has been solved by an adaptive fuzzy gain scheduling PID controller, based on a two-level architecture. The results of this scheme are corroborated through simulations showing that a maximum power operation can be reached under different conditions of solar radiation (considered as scheduled parameter).[7] The waste-waters reduction problem produced by oil industries has been solved through an adaptive gain scheduling control.[8] A tutorial on airship modelling and gain-scheduling control addressing the relevant aspects in airship modelling and its dynamics under different flight conditions has been reported. This tutorial provides a step-by-step control design for path-tracking, showing its effectiveness under realistic wind disturbances.[9] A control based on gain scheduling for a phase-shifted PWM full-bridge converter shows the application of this methodology to power electronics systems.[10] A set of gain-scheduled controllers have been designed for a helicopter system[11] and, finally, a fuzzy gain scheduling control scheme for a permanent magnet synchronous motor has been reported.[12] From the works previously mentioned and from the point of view of the combination with different control schemes, the flexibility of the gain scheduling methodology can be concluded. Such a particular formulation is used in the present paper to design a riderless bicycle control system to maintain its upright position with an LPV model depending on the translational velocity of the vehicle (considered as scheduling parameter). In this direction, previous research related to the bicycle go from works which analyse its dynamical behaviour, to studies reflecting the impact of the vehicle on our daily life.[13-15] With respect to previous works on the control of the bicycle, a work dealing with the error tracking minimization for specific velocities has been developed by considering a method to ensure, for the rider, a desired velocity.[16] The bicycle, in the context of the mathematical modelling of its dynamical behaviour, has been broadly addressed. For instance, the mathematical model of a bicycle (controlled by a pedalling torque, a directional torque and a rotor mounted on the bicycle) rolling on a moving plane has been computed.[17-19] The motion of a bicycle, on the other hand, has been studied with the objective of knowing the effects of the rider when the vehicle is moving along a defined path, in order to generate results to be analysed through statistical tools.[20] The design of an adaptive neuro-fuzzy controller for a bicycle has been computed presenting, through simulation and experimental results, its effectiveness.[21] A control system with the objective of guaranteeing a defined path tracking, as well, has been reported.[22] The bicycle stabilization using a gyroscope controlled by a non-linear control scheme was studied too.[23] A controller based on a second-order sliding-mode has been presented for the stabilization of an intelligent bicycle.[24] The control algorithm for trajectory tracking and balancing of an autonomous motorcycle has been addressed with a non-linear controller designed to handle the vehicle balancing[25] and, finally, studies related to the riderless bicycle system from the point of view of fault diagnosis and isolation and fault tolerant control can be found.[26-28] As shown through the papers and research works previously mentioned, it is possible to conclude that the bicycle dynamics and gain scheduling techniques are considered as an important and interesting research topic in many different areas. Thus, the results presented in this paper are related to the stabilization of a riderless bicycle by a gain scheduling LQR (Linear Quadratic Regulator) control with integral action based on a Luenberger observer, aiming at its implementation on an instrumented prototype. The contribution of the results presented throughout this paper with respect to previous works are mainly referred to combination of LQR and gain scheduling methodologies, in order to design a stabilization control system to maintain upright position of the vehicle without a rider, when the vehicle is moving as a result of a decreasing time-varying translational velocity. The objective is reached by means of a set of linear controllers and a Luenberger observer depending on the local translational velocity value, corroborated through experimental results. The paper structure is as follows. Section 2 presents the definition of a polynomial LPV system, including the required tools to analyse its dynamical properties. Section 3 shows the riderless bicycle system definition, along with the controllability and observability conditions. Section 4 addresses the related to the proposed stabilization control system. Section 5 shows the riderless bicycle prototype instrumentation and the corresponding experimental results. Section 6 presents a discussion and a brief conclusion is presented in Section 7.

Polynomial LPV systems

This Section presents the definition of polynomial LPV systems along with their structural properties. Consider the following dynamical system:

$$\dot{x} = A(\Theta(t))x + B(\Theta(t))u$$
$$y = C(\Theta(t))x \tag{1}$$

where $x \in \mathbb{R}^n$, $u \in \mathbb{R}^p$ and $y \in \mathbb{R}^s$ correspond the state, input and output, respectively. $A(\Theta(t))$, $B(\Theta(t))$ and $C(\Theta(t))$ are parameter-dependent matrices of compatible dimensions with $\Theta(t) \in \mathbb{R}^m$ considered as the time-varying parameter vector. In general, it is assumed that $\Theta(t)$

is measurable and bounded. If $A(\Theta(t))$, $B(\Theta(t))$ and/or $C(\Theta(t))$ acquire the form:

$$\chi(\Theta(t)) = \chi_0 + \sum_{i=1}^{k} \sum_{j=1}^{m} \chi_{\{[(i-1)m]+j\}} \Theta(t)_j^i \quad (2)$$

for some $k \geq 1$, where χ_l, $l = 0, \ldots, km$, are matrices of compatible dimensions (depending on the referred matrix $A(\Theta(t))$, $B(\Theta(t))$ or $C(\Theta(t))$), then the model (1) is a polynomial LPV system. From now on, the argument t will be dropped for sake of simplicity. In relation to the structural properties for LPV systems, the controllability and observability conditions can be seen as the extension of these criteria applied to LTI systems.[29] The polynomial LPV system (1), considering the representation (2), is controllable if:

$$rank[B(\Theta) \ A(\Theta)B(\Theta) \ldots A(\Theta)^{n-1}B(\Theta)] = n \ \forall \ \|\Theta\| \tag{3}$$

In analogous way, a polynomial LPV system will be observable if:

$$rank \begin{bmatrix} C(\Theta) \\ C(\Theta)A(\Theta) \\ \vdots \\ C(\Theta)A(\Theta)^{n-1} \end{bmatrix} = n \ \forall \ \|\Theta\| \tag{4}$$

Riderless bicycle dynamical system

The riderless bicycle model can be computed from the decomposition of the physical system in three bodies: i) a general frame, ii) a front frame composed by the handlebar and its corresponding oriented wheel and iii) the tires.[30−31] The dynamics of the system is approximated by the following general equation.

$$H\ddot{q} + vW\dot{q} + (gE_0 + v^2E_1)q = f \tag{5}$$

In equation (5), q is an angular position vector containing the roll angle ϕ and the handlebar angle δ, i.e. $q = [\phi \ \delta]^T$. The roll angle ϕ represents the position of the general frame with respect to the vertical position of the bicycle. The handlebar angle δ, on the other hand, corresponds to the angle formed by the handlebar and its perpendicular position with respect to the general frame. The general input forces acting into the system correspond to a torque applied to the handlebar T_δ and a torque applied to the general frame T_ϕ. The variables T_δ and T_ϕ are considered within the vector $f = [T_\delta \ T_\phi]^T$, as shown in Figure 1.
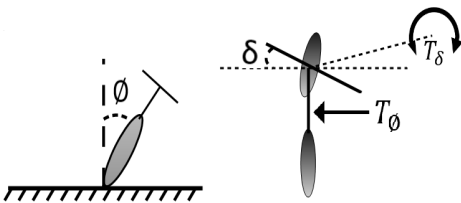

Figure 1. Riderless bicycle: front view (left) and top view (right)

In equation (5), W and H are the damping and mass matrices, respectively. Finally, E_0 and E_1 represent stiffness coefficients, the parameter g captures the gravity acceleration and v is the translational velocity of the vehicle. In order to compute the state-space representation for the riderless bicycle system, notice that equation (5) can be rewritten as:

$$\ddot{q} = H^{-1}f - H^{-1}(vW\dot{q}) - H^{-1}(gE_0 + v^2E_1)q \tag{6}$$

where:[30−31]

$$W = \begin{bmatrix} W_{11} & W_{12} \\ W_{21} & W_{22} \end{bmatrix} \quad E_0 = \begin{bmatrix} E_{011} & E_{012} \\ E_{021} & E_{022} \end{bmatrix} \tag{7}$$

$$H = \begin{bmatrix} H_{11} & H_{12} \\ H_{21} & H_{22} \end{bmatrix} \quad E_1 = \begin{bmatrix} 0 & E_{112} \\ 0 & E_{122} \end{bmatrix} \tag{8}$$

By defining the state vector as $x = [q \ \dot{q}]^T = [\phi \ \delta \ \dot{\phi} \ \dot{\delta}]^T$, the following is obtained:

$$\dot{x} = \begin{bmatrix} 0 & 0 & 1 & 0 \\ 0 & 0 & 0 & 1 \\ \bar{E}_{011} & \bar{E}_{012} - \bar{E}_{112}v^2 & \bar{W}_{11}v & \bar{W}_{12}v \\ \bar{E}_{021} & \bar{E}_{022} - \bar{E}_{122}v^2 & \bar{W}_{21}v & \bar{W}_{22}v \end{bmatrix} x \tag{9}$$

where $\bar{W}_{mn}$ corresponds to the product of $H^{-1}W$, $\bar{E}_{0mn}$ $m = n = 1, 2$ is the product of $H^{-1}gE_0$ and $\bar{E}_{1mn}$ define the matrix operation $H^{-1}E_1$. Going on with the system definition, by taking $u = T_\delta$ as unique input force $f = [T_\delta \ 0]^T$:

$$\begin{bmatrix} 0 \\ 0 \\ \bar{f}_{11} \\ \bar{f}_{21} \end{bmatrix} T_\delta \tag{10}$$

where $\bar{f}_{o1}$ $o = 1, 2$ is the product of $H^{-1}f$ and, finally, including equations (9)-(10) within a single expression as well as the output vector $y = [\delta \ \dot{\phi}]^T$ with $\Theta = v$ in equation (1), the state-space representation for the system can be represented as:

$$\begin{aligned} \dot{x} &= A(v)x + Bu \\ y &= Cx \end{aligned} \tag{11}$$

with the following matrices defined as:[32−33]

$$A(v) = \begin{bmatrix} 0 & 0 \\ 0 & 0 \\ 13.67 & 0.225 - 1.319v^2 \\ 4.857 & 10.81 - 1.125v^2 \end{bmatrix}$$

$$\begin{matrix} 1 & 0 \\ 0 & 1 \\ -0.164v & -0.552v \\ 3.621v & -2.388v \end{matrix} \quad B = \begin{bmatrix} 0 \\ 0 \\ -0.339 \\ 7.457 \end{bmatrix} \tag{12}$$

The matrices E_0, E_1, H and W, giving rise to equations (9)-(10), depend on the physical and geometric properties of the instrumented prototype. Let us point out that the matrix $A(v)$ can be represented as $A(v) = A_0 + A_1v + A_2v^2$, which is congruent with a polynomial LPV system (equation 2 with $\Theta = v$). Figure 2 shows the open-loop eigenvalues considering a translational velocity variation from 0 to 3 m/s. The gray asterisks represent those eigenvalues with positive real part, while the rest correspond to eigenvalues with negative real part.
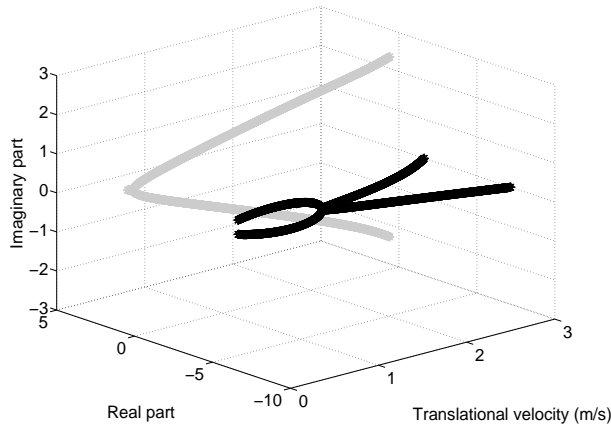
Figure 2. Open-loop eigenvalues as a function of the translational velocity v

Controllability and observability conditions

In order to compute the control system, it is important to analyse, before its design, the structural properties of the model. For the controllability condition (see equation (3) with $\Theta = v$), we follow the next procedure (where $|\cdot|$ represents the determinant of a matrix):

$$\Lambda_c(v) = |B \ A(v)B \ A(v)^2 B \ A(v)^3 B|$$
$$\Lambda_c(v) = -5806.5321v^4 + 19463.1274v^2 - 22.3115 \tag{13}$$

By getting the positive real roots of $\Lambda c(v)$, we get the following set for the translational velocity where controllability is lost:

$$\lambda_c = \{0.03386, 1.8305\} \tag{14}$$

As for the observability condition, it can be computed from the transpose of equation (4) with $\Theta = v$ since $rank[\sigma] = rank[\sigma^T]$ (where σ is a given matrix). Let us point out that equation (4) will result in a translational velocity dependent rectangular matrix. As a result, the transpose of (4), represented as $\Lambda_o(v)$, is:

$$\Lambda_o(v) = \begin{bmatrix} 0 & 0 & 0 & 13.67 & 4.857 \\ 1 & 0 & 0 & 0.225 - 1.319v^2 & 10.81 - 1.125v^2 \\ 0 & 1 & 0 & -0.164v & 3.621v \\ 0 & 0 & 1 & -0.552v & -2.388v \end{bmatrix}$$

$$\begin{matrix} -4.922v & 37.9v \\ 0.837v^3 - 6v & -2.089v^3 - 24.996 \\ 13.67 - 1.971v^2 & 4.857 - 9.240v^2 \\ 0.089v^2 + 0.225 & 2.578v^2 + 10.81 \end{matrix}$$

$$\begin{matrix} 187.961 - 26.520v^2 \\ 2.5v^4 - 17.758v^2 + 5.51 \\ 0.648v^3 - 6.350v \\ 1.711v^3 - 14.087v \end{matrix} \Bigg] \tag{15}$$

In order to compute $rank[\Lambda_o(v)] = rank[\Lambda_o(v)^T]$, the procedure begins with a non-zero determinant operation considering a square matrix of $n - 1$ dimension. Once this has been solved, the remaining rows and columns, to obtain matrices of $n \times n$ dimension, are incorporated. For each square matrix, the determinant operation is computed. Let

us point out that the determinant operation will result in an equation depending on the time-varying parameter v. Thus, $\forall v$ such that $rank[\Lambda_o(v)] \neq n$, the LPV model is not observable. By computing the previous procedure, the observability of the riderless bicycle model is concluded $\forall v$, since a coincident value for v does not exists in all solutions. As a result, the analysis of controllability and observability conditions allow to define the following translational velocity interval for the bicycle for practical purposes:

$$\Phi := [1.85, 3] \tag{16}$$

where the translational velocity is expressed in m/s. Φ is the range for v where the controllability and observability conditions are not lost.

Stabilization control system

Once the time-varying parameter range has been defined to ensure the controllability and observability conditions, the stabilization control system for the riderless bicycle can be designed. The control objective consists in guaranteeing the upright position of the vehicle in spite of the variation of the translational velocity v along a defined path. For this to be achieved, the following control law is proposed:

$$u = T_\delta = -K_i(v)x_i - K(v)\hat{x} \tag{17}$$

where $K_i(v)$ is the integral control gain depending on the time-varying parameter and $x_i = \int (r - \hat{\phi})dt$ represents the integer action applied to the error tracking $r - \hat{\phi}$. The reference signal to be followed is defined as r and $\hat{\phi}$ is the estimation of the controlled variable provided by a Luenberger observer. $K(v)$ is the stabilizing time-varying control gain. Figure 3, as a reference for the control system explanation, shows the closed-loop system. Let us point out that the control law (17) is composed by two terms: an integral action applied to the controlled variable $\hat{\phi}$ and a stabilizing action for the estimated system state $\hat{x}$.
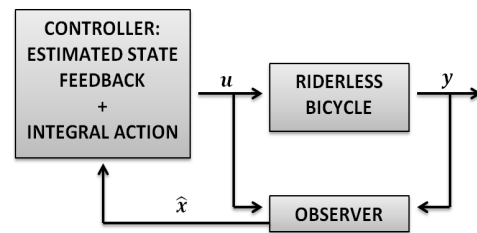
Figure 3. General block diagram of the closed-loop system

Thus, as shown in equation (17), an observer in charge of the system state estimation is needed: a Luenberger observer has been selected:

$$\dot{\hat{x}} = A(v)\hat{x} + Bu + L(v)(y - \hat{y}) \tag{18}$$

where $\hat{x}$ is the estimation of x and $L(v)$ is the time-varying observer gain. y and $\hat{y}$ correspond to the system output and estimated system output, respectively. By defining the estimation error variable as $e_e = x - \hat{x}$, the estimation error dynamics adopts the form:

$$\begin{aligned}
\dot{e}_e &= \dot{x} - \dot{\hat{x}} \\
&= A(v)(x - \hat{x}) - L(v)C(x - \hat{x}) \\
&= (A(v) - L(v)C)e_e
\end{aligned} \quad (19)$$

where $L(v)$ will be in charge of the estimation error convergence ensuring that $\hat{x} \rightarrow x \; \forall v \in \Phi$ as $t \rightarrow \infty$. Let us define an additional state:

$$\dot{x}_i = r - \hat{\phi} \quad (20)$$

which corresponds to $x_i = \int(r - \hat{\phi})dt$: the integral action applied to the tracking error. Thus, considering equations (11) and (17), the closed-loop system will be:

$$\dot{x} = A(v)x + B(-K_i(v)x_i - K(v)\hat{x}) \quad (21)$$

from $\hat{x} = x - e_e$:

$$\begin{aligned}
\dot{x} &= A(v)x - BK_i(v)x_i - BK(v)\hat{x} \\
&= A(v)x - BK(v)(x - e_e) - BK_i(v)x_i \\
&= (A(v) - BK(v))x + BK(v)e_e - BK_i(v)x_i
\end{aligned} \quad (22)$$

Going on with the stabilization control system design, $\hat{\phi} = \tilde{C}\hat{x}$ with $\tilde{C} = [1 \; 0 \; 0 \; 0]$:

$$\begin{aligned}
\dot{x}_i &= r - \hat{\phi} \\
&= r - \tilde{C}\hat{x} \\
&= r - \tilde{C}x + \tilde{C}e_e
\end{aligned} \quad (23)$$

and finally, by taking the estimation error $\dot{e}_e$ (equation (19)), the closed-loop system $\dot{x}$ (equation (22)) and $\dot{x}_i$ (equation (23)), the following is obtained.

$$\begin{bmatrix} \dot{x} \\ \dot{x}_i \\ \dot{e}_e \end{bmatrix} = \begin{bmatrix} A(v) - BK(v) & -BK_i(v) \\ -\tilde{C} & 0 \\ 0 & 0 \\ BK(v) \\ \tilde{C} \\ A(v) - L(v)C \end{bmatrix} \begin{bmatrix} x \\ x_i \\ e_e \end{bmatrix} + \begin{bmatrix} 0 \\ 1 \\ 0 \end{bmatrix} r \quad (24)$$

In equation (24), the dynamics in the proposed control scheme have been incorporated within a single expression, giving rise to the closed-loop system depicted in Figure 4.

Figure 4. Block diagram of the closed-loop system

Let us point out that the reference signal r will be 0 in the presented context, since the model (11) is valid for small variations around the upright position of the bicycle. In other words, the reference r must be zero in order to guarantee the vertical position of the bicycle, under the consideration that

the augmented state x_i will be continuously integrating the controlled variable $\hat{\phi}$. Going on with the controller design, equation (24) can be represented as:

$$\begin{bmatrix} \dot{X} \\ \dot{e}_e \end{bmatrix} = \begin{bmatrix} \tilde{A}(v) & \Delta(v) \\ 0 & A(v) - L(v)C \end{bmatrix} \begin{bmatrix} X \\ e_e \end{bmatrix} \quad (25)$$

with:

$$X = \begin{bmatrix} x \\ x_i \end{bmatrix} \quad \tilde{A}(v) = \begin{bmatrix} A(v) - BK(v) & -BK_i(v) \\ -\tilde{C} & 0 \end{bmatrix}$$
$$\Delta(v) = \begin{bmatrix} BK(v) \\ \tilde{C} \end{bmatrix} \quad (26)$$

From equation (25), the linearity separation principle is accomplished. This can be interpreted in the sense that, by designing a proper observer gain $L(v)$, the term $e_e \rightarrow 0$ as $t \rightarrow \infty$ and, consequently, $\Delta(v)$ will not have influence in the design of the control gains $K(v)$ and $K_i(v)$. In other words, a proper $L(v)$ will result in the elimination of the term e_e, resulting in the possibility of the controller design and observer design in independent way.

Control law design

For the control gain let us point out that $\tilde{A}(v)$ in equation (26) can be represented as:

$$\begin{aligned}
\tilde{A}(v) &= \begin{bmatrix} A(v) - BK(v) & BK_i(v) \\ -\tilde{C} & 0 \end{bmatrix} \\
&= \begin{bmatrix} A(v) & 0 \\ -\tilde{C} & 0 \end{bmatrix} - \begin{bmatrix} B \\ 0 \end{bmatrix} [K(v) \; Ki(v)]
\end{aligned} \quad (27)$$

Thus, as explained in previous Sections, an LQR control considering equation (27) can be designed directly using standard tools. The control gain computation will be addressed in later Sections.

Observer design

In addressing the linear separation principle from equation (25), the observer design begins by considering the dynamics of the estimation error e_e:

$$\dot{e}_e = (A(v) - L(v)C)e_e \quad (28)$$

It is necessary to find $L(v)$ that guarantees the estimation error convergence for any v i.e., an observer gain $L(v)$ such that $e_e \rightarrow 0$ as $t \rightarrow \infty \; \forall v \in \Phi$. For this to be achieved, a Lyapunov stability analysis has been developed. Consider the Lyapunov function candidate $V = e_e^T P e_e$ with $P = P^T > 0$:

$$\begin{aligned}
\dot{V} &= e_e^T P \dot{e}_e + \dot{e}_e^T P e_e \\
&= e_e^T [P(A(v) - L(v)C)e_e] + \\
&\quad \{[(A(v) - L(v)C)e_e]^T P\}e_e \\
&= e_e^T [PA(v) - PL(v)C + A(v)^T P - C^T L(v)^T P]e_e
\end{aligned} \quad (29)$$

As a result, equation (29) presents a bilinear condition due to the product $PL(v)$ and $[PL(v)]^T$. This is because both terms, P and $L(v)$, are decision variables involved in the

LMI. In order to eliminate this condition, by defining $\tilde{L}(v) = PL(v)$ and consequently $\tilde{L}(v)^T = L(v)^T P$, the following is obtained:

$$\dot{V} = e_e^T[PA(v) - \tilde{L}(v)C + A(v)^T P - C^T\tilde{L}(v)^T]e_e \tag{30}$$

Finally, if $\exists\, P = P^T > 0$ such that:

$$PA(v) - \tilde{L}(v)C + A(v)^T P - C^T\tilde{L}(v)^T < 0 \tag{31}$$

the observer gain $L(v) = P^{-1}\tilde{L}(v)$ guarantees the estimation error convergence and, as a result, $\hat{x} \to x$ as $t \to \infty$. Finally, with $L(v)$, the estimation of $\hat{x}$ allows the control law computation. As an additional restriction, an LMI region has been considered,[34] in order to ensure a fast and non-oscillating response for the estimated system state. The LMI region is formulated as:

$$PA(v) - \tilde{L}(v)C + A(v)^T P - C^T\tilde{L}(v)^T + 2P\alpha < 0 \tag{32}$$

and:

$$\begin{bmatrix} \sin\theta(A_o(v) + A_o(v)^T) & \cos\theta(A_o(v) - A_o(v)^T) \\ \cos\theta(A_o(v)^T - A_o(v)) & \sin\theta(A_o(v) + A_o(v)^T) \end{bmatrix} < 0 \tag{33}$$

where $A_o(v) = PA(v) - \tilde{L}(v)C$. The LMI region presented in equation (32) will allocate the eigenvalues of $A(v) - L(v)C$ in the left side of the value α within the complex plane. The parameter θ, on the other hand, defines a conic region in terms of the angle θ with respect to the real axis on the left side of the complex plane. As a result, the observer gain $L(v)$ will be computed by solving equations (31)-(33) simultaneously.

Control and observer gains computation

In order to compute the control and observer gains, it is important to notice that equations (31)-(33) correspond to a LMI set depending on the time-varying parameter. These LMI restrictions are considered as an infinite problem (PLMI), due to the continuous translational velocity variation. To solve the problem and, because of the fact that the presented control methodology takes the operating point for the system as the adopted value for the time-varying parameter, by considering $v = jh$ where $j = 1, 2, \ldots, N$ and h represents the velocity range contained within two consecutive points, the control and observer gains can be computed. The previous procedure ensures the control and observer gains computation at each jh and, by applying an interpolation method, the continuous solution can be obtained.[1] Consequently, for the control gains computation, we define $v = jh$ and:

$$\begin{aligned} \tilde{A}(jh) &= \begin{bmatrix} A(jh) & 0 \\ -\tilde{C} & 0 \end{bmatrix} - \begin{bmatrix} B \\ 0 \end{bmatrix}[K(jh)\ Ki(jh)] \\ &= \bar{A}(jh) - \bar{B}\bar{K}(jh) \end{aligned} \tag{34}$$

As a result, from equation (34), the control gains can be computed by means of the LQR command provided by

MATLAB. This is done by selecting the weighting matrices Q and R. From equation (34), the LQR command computes the optimal control gain $K(jh)$ in such a way that $u = -K(jh)x$ minimizes the cost function:

$$J(u) = \int_0^\infty (x^T Q x + u^T R u)dt \tag{35}$$

The control gain $K(jh)$, as a consequence, is computed from:

$$K(jh) = R^{-1}(\bar{B}^T D(jh)) \tag{36}$$

where $D(jh)$ corresponds to the solution of the associated Riccati equation:

$$\begin{aligned} &\bar{A}(jh)^T D(jh) + D(jh)\bar{A}(jh) \\ &- (D(jh)\bar{B})R^{-1}(\bar{B}^T D(jh)) + Q = 0 \end{aligned} \tag{37}$$

In this paper, the control gain will be addressed at each performed test along with the matrices Q and R. The observer gain, on the other hand, has been computed by considering the following LMI set:

$$PA(jh) - \tilde{L}(jh)C + A(jh)^T P - C^T\tilde{L}(jh)^T < 0 \tag{38}$$

$$PA(jh) - \tilde{L}(jh)C + A(jh)^T P - C^T\tilde{L}(jh)^T + 2P\alpha < 0 \tag{39}$$

and:

$$\begin{bmatrix} \sin\theta(A_o(jh) + A_o(jh)^T) \\ \cos\theta(A_o(jh)^T - A_o(jh)) \\ \cos\theta(A_o(jh) - A_o(jh)^T) \\ \sin\theta(A_o(jh) + A_o(jh)^T) \end{bmatrix} < 0 \tag{40}$$

where $L(jh) = P^{-1}\tilde{L}(jh)$ and $A_o(jh) = PA(jh) - \tilde{L}(jh)C$. Equations (38)-(40) include the LMI region defined previously. Let us point out that, due to the measured outputs y, the observer gain can be represented as:

$$L(jh) = \begin{bmatrix} l_{11}(jh) & l_{12}(jh) & l_{13}(jh) & l_{14}(jh) \\ l_{21}(jh) & l_{22}(jh) & l_{23}(jh) & l_{24}(jh) \end{bmatrix}^T \tag{41}$$

Selecting $N = 230$, $h = 0.005$ and the parameters $\alpha = 6.5$ and $\theta = 0.025$ rad for the LMI region, Figures 5 and 6 present the computed observer gains. The observer gain, for this part, generates the eigenvalues for $A(jh) - L(jh)C$ depicted in Figure 7. In order to show the correct application of the considered LMI region, on the other hand, the asterisks in Figure 8 show the eigenvalues $\forall\ jh$. The observer gains where computed with MATLAB, YALMIP[36] and the solver SEDUMI. Finally, from Figures 7 and 8, the convergence for the state estimation error e_e is concluded.

Riderless bicycle prototype and experimental results

Riderless bicycle prototype

The riderless bicycle requires the measurements of the outputs δ and $\dot{\phi}$ as well as the translational velocity v. Moreover, a device capable to apply the control law T_δ is equally needed. This highlights the need of three sensors
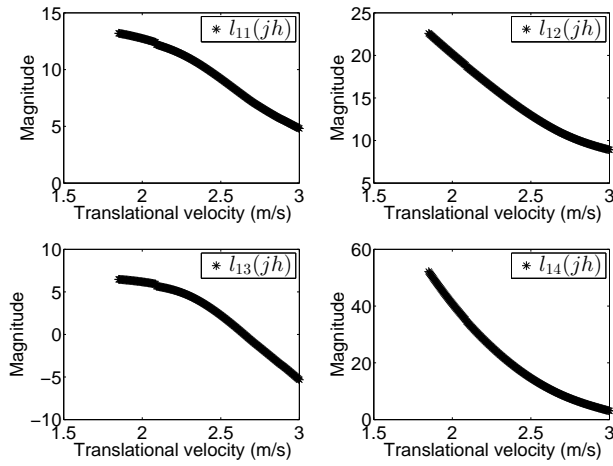
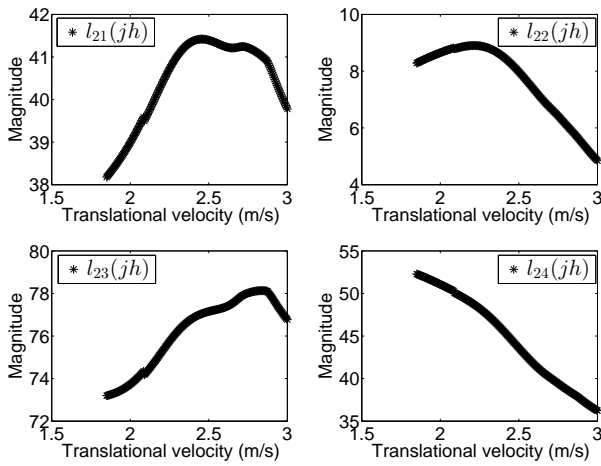**Figure 5.** Observer gains l_{1i}, $i = 1, \ldots, 4$

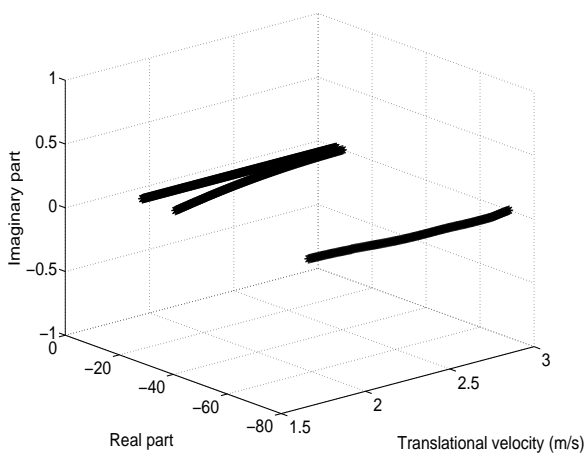**Figure 6.** Observer gains l_{2i}, $i = 1, \ldots, 4$

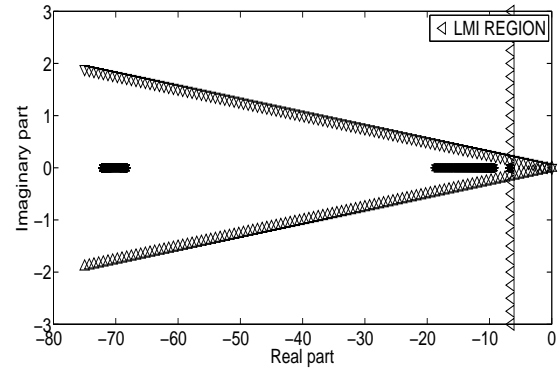**Figure 7.** Eigenvalues of $A(jh) - L(jh)C$

Figure 8. Real part of $A(jh) - L(jh)C$ eigenvalues

connections and interaction. The device in charge of the sensor signal acquisition (measurements) and the command signal generation for the system actuator is the PEC80 processing system, by ABB.
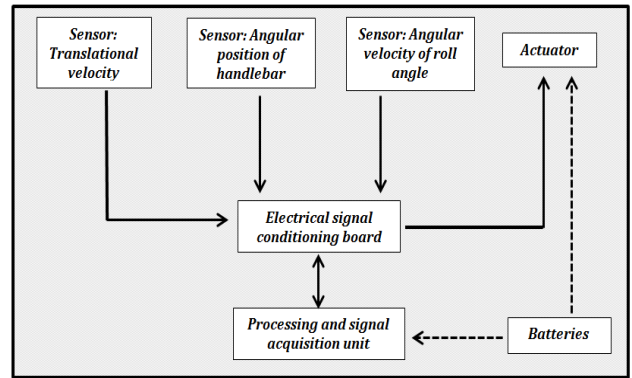

Figure 9. General schematic of the riderless bicycle instrumentation

The PEC80 controller (see Figure 10 label A) is a system specially designed for applications where the requirement of control tasks with high velocities is needed, mostly, within the power electronics field. The electronic board (Figure 10 label B) performs the signal conditioning to allow the correct communication between the sensors and the data acquisition unit, as well as the corresponding signal conditioning for the system actuator. The device in charge of the torque application to the handlebar (the control input in the mathematical model) is a servo-motor (Figure 10 label C). This servo-motor allows the change of the handlebar angular position, by using a metal piece coupled to the handlebar. For the measurement of the velocity of the roll angle $\dot{\phi}$, a gyroscope mounted in the general frame of the bicycle has been used (see Figure 10 label D). This signal is ready to be received into the acquisition unit. On the other hand, for the angular position of the handlebar, a potentiometer coupled to the servo-motor rotor has been incorporated. The potentiometer changes its resistance value depending on the servo-motor motion, which, in turn, is proportional to the handlebar position. Finally, for the translational velocity computation, a Hall effect built encoder with 36 ferrous metal plates placed on the periphery of the rear wheel has been considered (Figure 10 label E). This sensor generates a frequency when these plates passes on it.
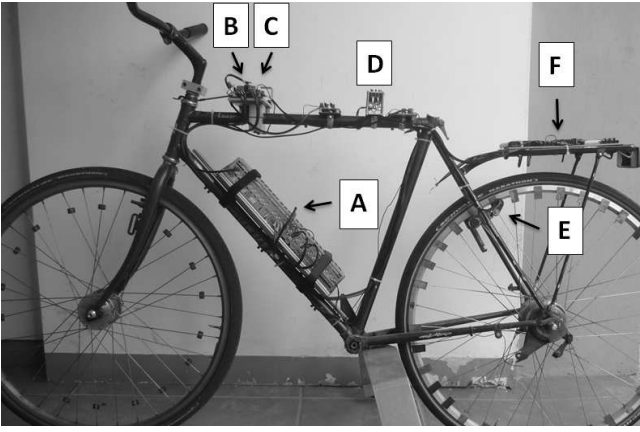
and one actuator. Additionally, the measured outputs should be introduced into a processing and signal acquisition unit, through an electronic board in charge of the electrical signal conditioning. Figure 9 presents the general components of the riderless bicycle instrumentation, in addition to their

Figure 10. Instrumented riderless bicycle

As a result, considering the number of plates, 36, the rear wheel radius (R_w) and the generated frequency (F), a routine programmed into the PEC computes the translational velocity for the bicycle. The complete instrumentation of the prototype is energized by means of a set of batteries placed on the rear part of the bicycle (Figure 10 label F).

Experimental results

Once the riderless bicycle prototype and the stabilization control system have been defined, it is possible to address the experimental implementation. For this, an internal function within the software allows to disable the control law when the translational velocity acquires values not included in Φ, or those values where the controllability and observability of the system are lost. Within the tests, the integral action considered in the control system is applied to $\hat{\phi}$ and $\hat{\delta}$. The first test involves the consideration of an integral action on $\hat{\phi}$ by taking $\tilde{C} = [1 \ 0 \ 0 \ 0]$ in equation (34). The weighting matrix Q was selected to be:

$$Q = \begin{bmatrix} I^{2\times2} & 0^{2\times1} & 0^{2\times2} \\ 0^{1\times2} & 500 & 0^{1\times2} \\ 0^{2\times2} & 0^{2\times1} & I^{2\times2} \end{bmatrix} \qquad (42)$$

where $I^{\eta\times\eta}$ stands for the identity matrix of $\eta \times \eta$ dimension, $0^{\eta\times\gamma}$ is a $0^{\eta\times\gamma}$ matrix whose elements are all zero, and $R = 1$. The weighting matrix Q contains a value 500 applied to the state $\dot{\phi}$, imposing more importance to one of the measured variables. Its value was empirically set from the fact that the measured variable $\dot{\phi}$ is directly involved in the controlled variable ϕ. For the control gains, the same parameters h and N have been considered as in the observer gains, computed with MATLAB and its LQR command. The computed control gains are depicted in Figure 11 by considering $K(jh) = [k_\phi(jh) \ k_\delta(jh) \ k_{\dot{\phi}}(jh) \ k_{\dot{\delta}}(jh))]$. Let us point out that the selection of the weighting matrix Q at the fifth row and fifth column corresponds to the weighting value imposed for the integral action $k_i(jh)$. Now, it is important to stand that the last row of equation (34) related to the integral action does not depend on the time-varying parameter, thus, the computed integral gain corresponds to a constant value. By considering the control gains depicted in Figure 11, the resulting closed-loop eigenvalues are shown in Figure 12.
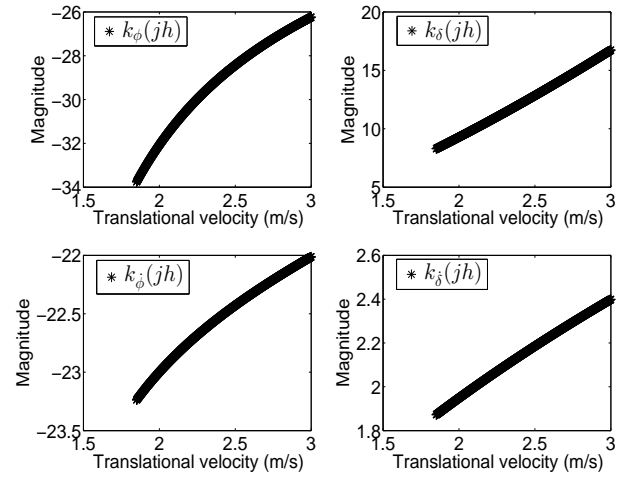

Figure 11. Control gains in experimental test considering $Q_{\dot{\phi}} = 500$
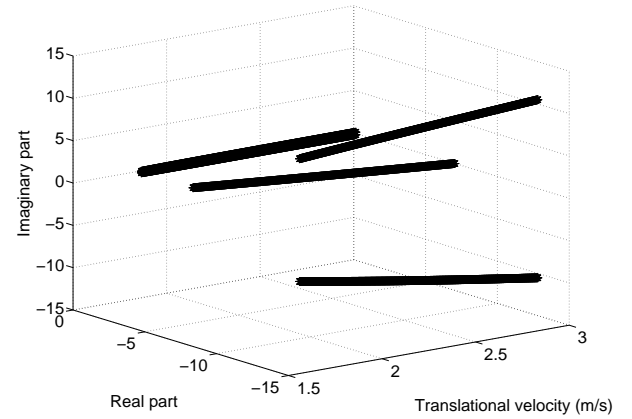

Figure 12. Closed-loop eigenvalues in experimental test considering $Q_{\dot{\phi}} = 500$

From Figure 12, two pairs of complex conjugate eigenvalues and a real eigenvalue can be seen. The first pair of complex conjugate eigenvalues goes from $-0.1893 \pm 0.0905i$ to $-0.1543 \pm 0.1443i$, the second pair has a variation from $-11.1986 \pm 7.2434i$ to $-12.825 \pm 10.5193i$ and, finally, the real eigenvalue takes values from -3.78940 to -7.0506. Indeed, the change of the closed-loop eigenvalues is because of the translational velocity variation. As a result, the stability of the closed-loop system is concluded from Figure 12. A video containing the experimental results (shown in Figure 13) for the selected parameters Q and R, can be watched in https://drive.google.com/open?id=0B3_lWyaVb2r1LVp5V1hWcUI3eU0. From Figure 13, an increasing translational velocity is seen (subplot e) from 2.1 m/s to 2.7 m/s in 6 s approximately. The controlled variable $\hat{\phi}$ is depicted in Figure 13a where its behaviour is close to the equilibrium point represented as 0 in the plots. Recall that the equilibrium point in the real context corresponds to the upright position of the bicycle. The subplot c in Figure 13 shows the steer angle δ manipulated through the control law T_δ, depicted in Figure 13f. The rest

of the plots (b and d) show the motion velocities for the roll angle and steer angle, respectively.
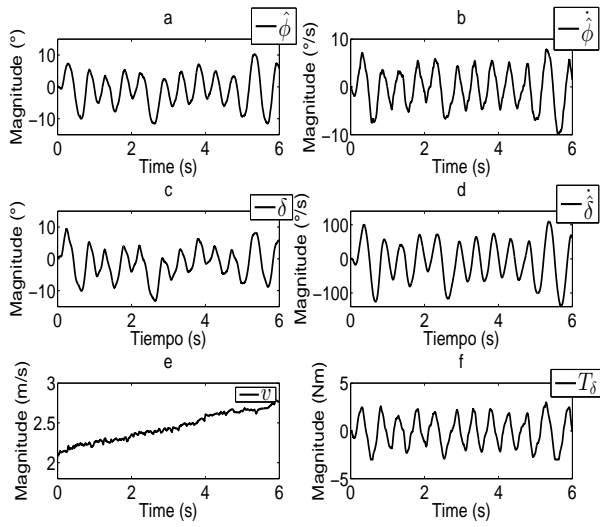

Figure 13. Result of experimental test considering $Q_{\dot{\phi}} = 500$

For the second test, an increase on the weighting matrix Q has been considered, by maintaining the same value for R as in the previous case. This is done in order to perceive a change on the control gains and, consequently, a different control law and a different dynamical evolution of the closed-loop system. The weighting matrix Q has been changed to:

$$Q = \begin{bmatrix} I^{2\times2} & 0^{2\times1} & 0^{2\times2} \\ 0^{1\times2} & 800 & 0^{1\times2} \\ 0^{2\times2} & 0^{2\times1} & I^{2\times2} \end{bmatrix} \tag{43}$$

The corresponding control gains are depicted in Figure 14.
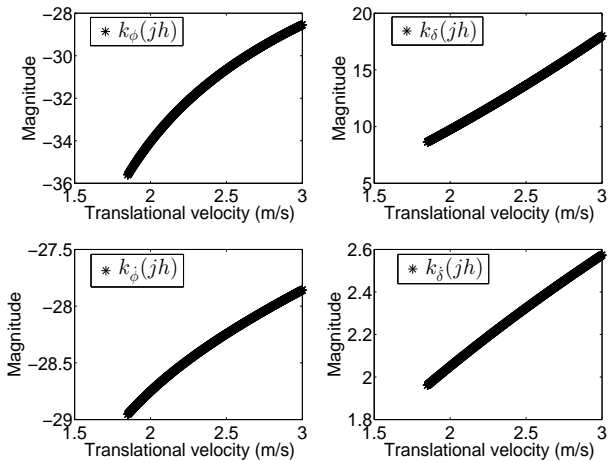
Figure 14. Control gains in experimental test considering $Q_{\dot{\phi}} = 800$

Let us point out a change in the magnitude of the control gain $k_{\dot{\phi}}$ which is consistent with the weighting matrix Q considered. The control gain k_ϕ has suffered a change as a consequence of the system structure, because of the fact that $\dot{\phi}$ will change the dynamical behaviour for its position ϕ. In order to force the system, the control gain for δ

should be changed too, in view of the consideration that the steer angle is the manipulated variable. Figure 15 presents the closed-loop eigenvalues considering the control gains depicted in Figure 14. As in the previous test, a pair of complex conjugated eigenvalues presents a variation from $-0.16 \pm 0.09i$ to $-0.13 \pm 0.12i$, a real eigenvalue goes from -3.78 to -7.02 and an additional pair of complex conjugated eigenvalues from -12.52 ± 8.16 to $-14.49 \pm 11.78i$.
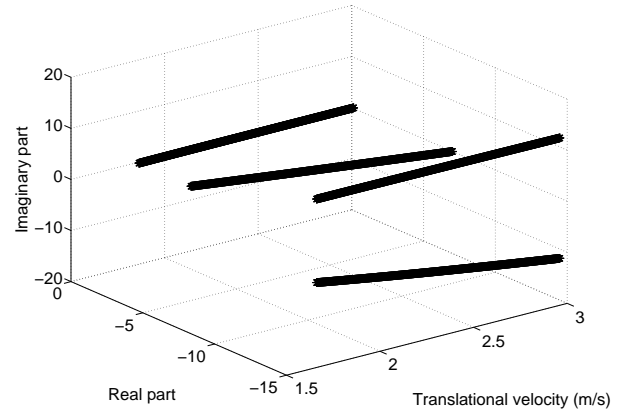

Figure 15. Closed-loop eigenvalues in experimental test considering $Q_{\dot{\phi}} = 800$

The experimental results for this test are presented in Figure 16 (https://drive.google.com/open?id=0B3_lWyaVb2r1NnRxT3ZPVFZ4V28). From Figure 16, the riderless bicycle control objective is reached while the translational velocity varies from an initial value of $2\ m/s$ towards $2.4\ m/s$. Let us point out that the increase on the translational velocity (time-varying parameter) takes place due to the testing ground conditions, with a negative slope. The controlled variable $\hat{\phi}$ is depicted in Figure 16a, maintaining its value around 0 with a less oscillating dynamical behaviour with respect to the previous test. As for the control law T_δ, shown in Figure 16f, an internal saturation for this variable is included as part of the software in the PEC controller, in order to prevent damages in the actuator (at $t \approx 2.1$ s). The rest of the plots have the same interpretation as in the previous test. Finally, the last test is presented considering the application of the integral control to the manipulated variable δ, in order to evaluate the effectiveness of the proposed stabilization control system. This is done by taking $\tilde{C} = [0\ 1\ 0\ 0]$ in equation (34). The weighting matrix Q was selected to be:

$$Q = \begin{bmatrix} 250 & 0 & 0 & 0 & 0 \\ 0 & 1 & 0 & 0 & 0 \\ 0 & 0 & 250 & 0 & 0 \\ 0 & 0 & 0 & 1 & 0 \\ 0 & 0 & 0 & 0 & 1 \end{bmatrix} \tag{44}$$

Figure 17 shows the computed control gains for the final test. From equation (44), a strong influence in the control gain computation for the variable ϕ and its velocity $\dot{\phi}$ have been specified. Figure 18, on the other hand, presents the closed-loop eigenvalues by using the resulting control gains.
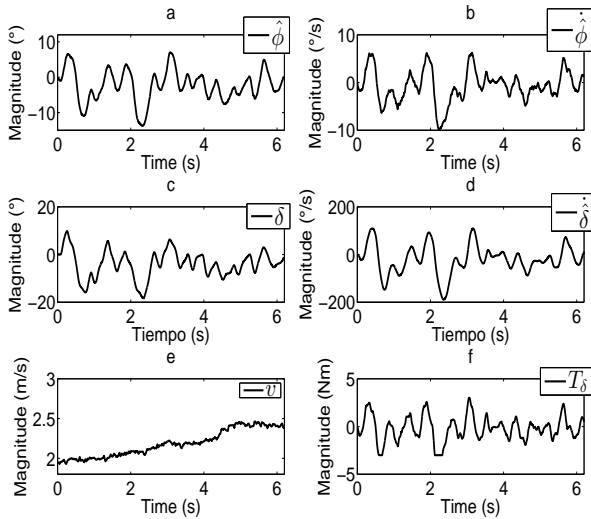
Figure 16. Result of experimental test considering $Q_{\dot{\phi}} = 800$
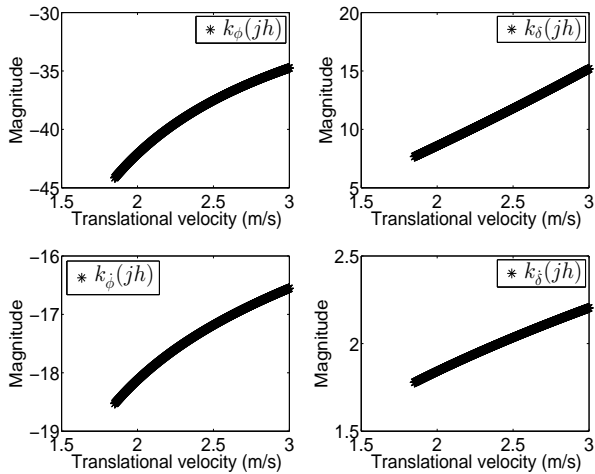

Figure 17. Control gains in experimental test considering integral action on the manipulated variable
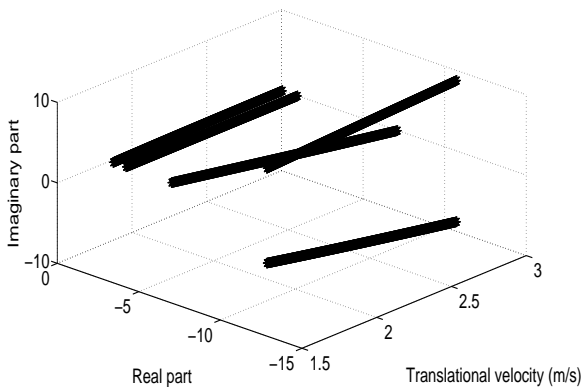

Figure 18. Closed-loop eigenvalues in experimental test considering integral action on the manipulated variable

From Figure 18 a pair of complex conjugated eigenvalues go from $-9.62 \pm 5.86i$ to $-10.74 \pm 8.78i$ and a set of three real eigenvalues can be seen. A constant one allocated

at -1, a second one varying from -7.12 to -3.75 and the final one varying from -0.2 to -0.1. The closed-loop response for the controlled system considering the integral action applied to the manipulated variable is presented in Figure 19. A small change of the translational velocity can be seen in Figure 19, varying slowly from $2.1\ m/s$ to $2.4\ m/s$. Let us point out that the controlled variable remains closer to the equilibrium point than the results seen in the previous tests. This is due to the integral action, since it is applied to the steer angle δ; or the manipulated variable https://drive.google.com/open?id=0B3_lWyaVb2r1OUlGU19wYmpfa3c.
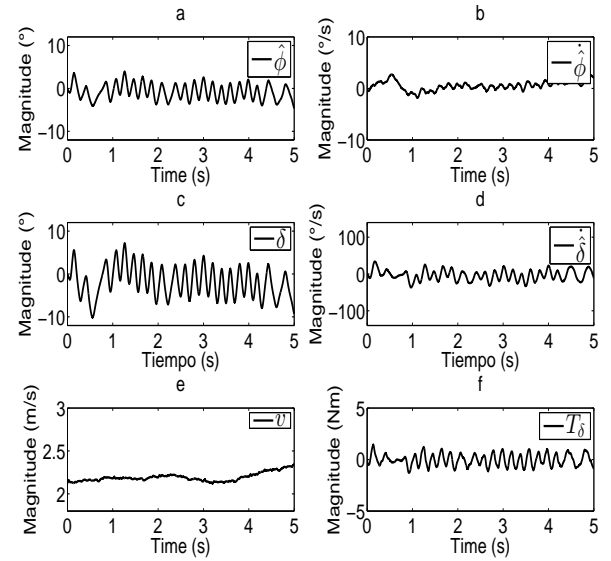

Figure 19. Result of experimental test considering integral action on the manipulated variable

Discussion

In this Section, a few comments about the presented results are provided. This is done from the theoretical point of view, in terms of the difference between the addressed methodology and the one considered for the well-know Linear Parameter Varying (LPV) systems. Let us point out that the gain scheduling methodology introduces a time-varying parameter in charge of the operating point definition, for the system. A drawback of this comes from the fact that the variation between a specific operating point and the coming one is not taken into account within the stability analysis. Further, the variation of this parameter can be such that the closed-loop stability for the controlled system is compromised. In order to retrieve the previously condition, the Linear Parameter Varying methodology is worth to be commented. This methodology, unlike gain scheduling, takes into account the variation of the time varying parameter within the Lyapunov stability analysis. In general terms, this is done by the consideration of a Lyapunov function depending on the time-varying parameter(s). As a result, a term representing the velocity variation of the time-varying parameter(s) appears into the derivative of the Lyapunov function, along the closed-loop

system trajectories. Consequently, the control scheme will be able to deal with a closed-loop system varying in terms of the parameter(s) considering a maximum value for its(their) velocity(ies). This is the main difference between the LPV stability analysis and the gain scheduling analysis. As a conclusion if the time varying parameter varies slowly, then a gain scheduled control system can be considered, as in the case in the presented results.

Conclusion

The present paper addresses the design of a gain scheduling control with the objective of the stabilization of a LPV system, with a riderless bicycle study case. The riderless bicycle LPV model acquires a high order time-varying dependency, parameter considered as the translational velocity of the vehicle. Throughout this work, the proposed control scheme was evaluated through experimental results, corroborating the effectiveness of the proposed control scheme. The main contribution of this paper corresponds to the riderless bicycle stabilization towards its upright position considering a time-varying translational velocity by a two-level controller, and the combination of the LQR and gain scheduling control methodologies. The regulation is performed by integral action applied to the controlled variable and the manipulated variable, the stabilization level, on the other hand, aims at reaching the convergence of the system state to the desired equilibrium. From the experimental results shown, the effectiveness of the proposed scheme has been corroborated, leading future works in terms of a desired velocity tracking.

References

1. Rugh WJ and Shamma JS. Research on gain scheduling. Automatica 2000; 36(10): 1401-1425.
2. Sato M. and Peaucelle D. Gain-scheduled output-feedback controllers using inexact scheduling parameters for continuous-time LPV systems. Automatica 2013; 49(4): 1019–1025.
3. Sato M. Gain scheduled state feedback controllers for discrete-time LPV systems using schedulling parameters affected by absolute and proportional uncertainties. IFAC-PapersOnLine 2015; 48(26): 31–36.
4. Balini HMNK, Witte J, Scherer CW. Synthesis and implementation of gain-scheduling and LPV controllers for an AMB system. Automatica 2012; 48(3): 521-527.
5. Han Y and Pan W. Gain-scheduled continuous higher-order sliding mode control for uncertain nonlinear system. Optik 2016; 127(10): 4345-4354.
6. Bedouda K, Ali-rachedic M, Bahi T, et al. Adaptive Fuzzy Gain Scheduling of PI Controller for control of the Wind Energy Conversion Systems. Energ Proc 2015; 74: 211-225.
7. Dounis AI, Kofinas P, Alafodimos C, et al. Adaptive fuzzy gain scheduling PID controller for maximum power point tracking of photovoltaic system. Renew energ 2013; 60: 202–214.
8. Fernandes LSL, Moraes-Filho FC, Paulo JBA, et al. Gain scheduling adaptive control applied to a particular mixer-settler equipment. Control Eng Pract 2013; 21(8): 1121-1127.
9. Moutinho A, Azinheira JR, de Paiva EC, et al. Airship robust path-tracking: A tutorial on airship modelling and gain-scheduling control design. Control Eng Pract 2013; 50: 22-36.

10. Chen CC, Chen CL, Chang JX, et al. LPV Gain-scheduling Control for a Phase-shifted PWM Full-bridge Soft Switched Converter. In: 19th IFAC World Congress, Cape Town, South Africa, August 24-29, 2014, 47(3): 6135–6140.
11. Prempain E and Postlethwaite I. A new two-degree-of-freedom gain scheduling method applied to the Lynx MK7. P I Mech Eng I-J Sys 2000; 214(4): 299–311.
12. Chang YH, Lin HW, Hu YH, et al. Fuzzy-scheduling control of a linear permanent magnet synchronous motor with payload variations. P I Mech Eng I-J Sys 2008; 222(6): 465–479.
13. Mendes M, Duarte G and Baptista P. Introducing specific power to bicycles and motorcycles: Application to electric mobility. Transport Res C-Emer 2015; 51: 120–135.
14. Baker SA and Calhoun VD. A custom bicycle handlebar adaptation for children with below elbow amputations. J Hand Ther 2014; 27(3): 258–260.
15. Roman M and Roman M. Bicycle Transport as an Opportunity to Develop Urban Tourism Warsaw Example. P Soc Behav Sci 2014; 151: 295–301.
16. Abagnale C, Cardone M, Iodice P, et al. Model-based control for an innovative power-assisted bicycle 2015. Energ Proc; 81: 606–617.
17. Yavin Y. Modelling and control of the motion of a riderless bicycle rolling on a moving plane. Comput Math Appl 2007, Vol. 54(11-12): 1319–1328.
18. Yavin Y. The Derivation of a Kinematic Model from the Dynamic Model of the Motion of a Riderless Bicycle. Comput Math Appl 2006; 51(6-7): 865–878.
19. Yavin Y. Stabilization and control of the motion of an autonomous bicycle by using a rotor for the tilting moment. Comput Math Appl 1999; 178(3-4): 233–243.
20. Moore JK, Hubbarda M, Schwabb AL, et al. Statistics of Bicycle Rider Motion. Proc Eng 2010; 2: 2937–2942.
21. Shafiekhani A, Mahjoob MJ and Akraminia M. Design and implementation of an adaptive critic-based neuro-fuzzy controller on an unmanned bicycle. Mechatronics 2015; 28: 115-123.
22. Edelmann J, Haudum M and Plöchl M. Bicycle Rider Control Modelling for Path Tracking. IFAC-PapersOnLine 2015; 48(1): 55–60.
23. Zhang Y, Wang P, Yi J, Song D, et al. Stationary Balance Control of a Bikebot. IEEE Int Conf Robot 2014; 6706–6711.
24. Defoort M and Murakami T. Sliding-Mode Control Scheme for an Intelligent Bicycle. IEEE T Ind Electron 2009; 56(9): 3357–3368.
25. Yi J, Song D, Levandowski A, et al. Trajectory Tracking and Balance Stabilization Control of Autonomous Motorcycles, IEEE Int Conf Robot 2006; 2583-2589.
26. Brizuela-Mendoza J.A., Astorga-Zaragoza C.M., Zavala-Río A, et al. State and actuator fault estimation observer design integrated in a riderless bicycle stabilization system. ISA T 2016; 61: 199-210.

27. Brizuela-Mendoza J.A., Astorga-Zaragoza C.M., Zavala-Río A, et al. Fault Tolerant Control for Polynomial Linear Parameter Varying (LPV) Systems applied to the stabilization of a riderless bicycle. European Control Conference (ECC), Zürich, Switzerland, July 17-19, 2013: 2957–2962.

28. Brizuela-Mendoza J.A., Astorga-Zaragoza C.M., Zavala-Río A, et al. Control Tolerante a Fallas Activo: Estimación y acomodación de fallas en sensores aplicado al modelo LPV de una bicicleta sin conductor Rev. Iberoam. Autom. Inf. Ind. 2016; 13: 174-185.

29. Briat C. Commande et Observation Robustes des Systèmes LPV Retardès. PhD Thesis, Grenoble IPN, FR, 2008.

30. Meijaard JP, Papadopoulos JM, Ruina A, et al. Linearized dynamics equations for the balance and steer of a bicycle: a benchmark and review. P Roy Soc A-Math Phy 2007; 463(2084): 1955–1982.

31. Schwab AL, Meijaard JP and Papadopoulos JM. Benchmark results on the linearized equations of motion of an uncontrolled bicycle. J Mech Sci Technol 2005; 19(1): 292–304.

32. Cerone V, Andreo D, Larsson M, et al. Stabilization of a riderless bicycle: a linear parameter varying approach. IEEE Contr Syst Mag 2010; 30(5): 23–32.

33. Andreo D, Cerone V, Dzung D, et al. Experimental results on LPV stabilization of a riderless bicycle. In: Proceedings of the American Control Conference, St. Louis, MO, USA June 10-12, 2009, paper no. ThB15.3, pp. 3124–3129.

34. Chillali M, Gahinet P and Apkarian P. Robust Pole Placement in LMI Regions. IEEE T Automat Contr 1999; 44(12): 2257–2270.

35. Löfberg J. YALMIP : a toolbox for modeling and optimization in MATLAB. In Proc of the CACSD Conf, Taipei, Taiwan September 2-4, 2004: 284–289.